Progress In Electromagnetics Research, Vol. 134, 79–94, 2013

HIERARCHICAL INTERPOLATIVE DECOMPOSITION MULTILEVEL FAST MULTIPOLE ALGORITHM FOR DYNAMIC ELECTROMAGNETIC SIMULATIONS

Xiaomin Pan* **and Xinqing Sheng**

Center for Electromagnetic Simulation, School of Information and Electronics, Beijing Institute of Technology, Beijing 100081, P. R. China

Abstract—A hierarchical interpolative decomposition multilevel fast multipole algorithm (ID-MLFMA) is proposed to handle multiscale, dynamic electromagnetic problems. The hierarchical scheme to conduct the ID skeletonization and to implement the matrix vector multiplication is discussed. A strategy to improve the efficiency of ID skeletonization is developed. The hierarchical ID-MLFMA are investigated by numerical experiments on complex targets, demonstrating the capability of the hierarchical ID-MLFMA.

1. INTRODUCTION

Efficient and accurate solutions of electromagnetic (EM) scattering and radiation problems have attained a lot of interest for decades. Among many full-wave numerical methods, the algorithms based on method of moments (MoM) have been widely used due to its high fidelity and superior capability to handle arbitrarily shaped targets. The computational complexity of MoM is $O(N^3)$ for a conventional direct solver in terms of CPU time, such as LU, and $O(mN^2)$ for an iterative algorithm, where N is the number of unknowns and m the iteration count. Consequently, rather than direct solvers, iterative ones in combination with some fast algorithms [1–9] are more popular in solving MoM systems. Most of these fast algorithms decompose interactions in MoM systems into near-field interactions (NFIs) and far-field interactions (FFIs), and then approximate FFIs in some efficient way. In these fast methods, FFIs are generally independent

Received 10 October 2012, Accepted 7 November 2012, Scheduled 21 November 2012

* Corresponding author: Xiaomin Pan (xmpan@bit.edu.cn).

of mesh size of the target of interest. Unfortunately, NFIs, always in the original MoM form, are highly dependent on the property of the mesh. As a result, fast methods will become inefficient for the so-called multiscale applications. In these cases, targets are over-meshed to conduct wide-band calculations, or partly over-meshed to capture the tiny geometrical structures.

Many efforts have been reported [10–13] (and references therein) to solve this problem. As pointed out in [10], the methods based on the evanescent wave expansion [11] or diagonalizations [12] require extra computational effort for evaluating the according translation operators with respect to the original MLFMA. The methods involving multipole expansions of Green's functions [2] show bad convergence behavior at low frequencies. In ID-MLFMA [13], these problems can be eliminated by the skeletonization approximation [14, 15]. In SVD/QR based methods [16], the original basis functions are linearly combined in the approximation. Contrarily, skeletons in ID-MLFMA are identical to their counterparts of basis/testing functions. A hierarchical scheme can be reached without many efforts to furtherly improve the generality and efficiency. Additionally, an effective algebraic preconditioner can be developed to accelerate the iterative solution since entries of the skeletonized matrix are selected from the original MLFMA NFI matrix. In this work, a hierarchical scheme is developed to perform the ID skeletonization. Based on the proposed scheme, a strategy of reducing the size of the low-rank matrix to select skeletons is proposed.

The rest of the paper is organized as follows. Section 2 begins with outlines of the conventional MLFMA and the previously developed ID-MLFMA. Section 3 discusses formulations on how to construct skeletons hierarchically and how to implement matrix-vector multiplication (MVM) in a hierarchical manner. Section 4 focuses on the mixed strategy to reduce the size of low-rank matrices. Section 5 presents some illustrative numerical results, and finally, a summary and some conclusions are given in Section 6.

2. MLFMA AND NON-HIERARCHICAL ID-MLFMA

2.1. MLFMA

For perfectly electric conducting (PEC) objects, discretization and testing of surface integral equations yields an $N \times N$ dense matrix equation in the form of

$$\mathbf{Z} \cdot \mathbf{I} = \mathbf{V}, \tag{1}$$

where $\mathbf{Z}$ is the impedance matrix; $\mathbf{I}$ relates with the unknown equivalent current; and $\mathbf{V}$ corresponds to the incident wave. In this

paper, both basis and testing functions are RWG functions. The matrix Equation (1) can be solved iteratively, and the required MVM can be accelerated by FMM or MLFMA [1, 2]. FMM/MLFMA decomposes MVM into NFIs and FFIs. The former is computed directly, while the latter is accelerated by FMM/MLFMA. The MVM in FMM reads

$$\mathbf{Z} \cdot \mathbf{I} = \mathbf{Z}_{\text{FMM-NFI}} \cdot \mathbf{I} + \mathbf{Z}_{\text{FMM-FFI}} \cdot \mathbf{I}, \tag{2}$$

with

$$\begin{aligned} \mathbf{Z}_{\text{FMM-FFI}} \cdot \mathbf{I} &= \sum_o \Big(\mathbf{D}_o \cdot \sum_{s \notin B_o} \mathbf{T}_{o,s} \cdot \mathbf{A}_s \cdot \mathbf{I}_s \Big), \\ \mathbf{Z}_{\text{FMM-NFI}} \cdot \mathbf{I} &= \sum_o \Big(\sum_{s \in B_o} \mathbf{Z}_{o,s} \cdot \mathbf{I}_s \Big), \end{aligned} \tag{3}$$

where $\mathbf{Z}_{o,s}$ is the impedance matrix corresponding to observation group o and source group s; $\mathbf{I}_s$ is the coefficient vector of RWG basis functions in group s; B_o denotes near neighbors of group o; $\mathbf{T}_{o,s}$ is the translator; $\mathbf{D}_o$ and $\mathbf{A}_s$ are the disaggregation and aggregation matrices. The term $\mathbf{Z}_{\text{FMM-NFI}} \cdot \mathbf{I}$ in (2) accounts for the contribution from the self-coupling of group o and its near neighbors. While the other one collects the contribution from remaining groups.

The MVM in MLFMA can be written as

$$\mathbf{Z} \cdot \mathbf{I} = \mathbf{Z}_{\text{MLFMA-NFI}} \cdot \mathbf{I} + \mathbf{Z}_{\text{MLFMA-FFI}} \cdot \mathbf{I}. \tag{4}$$

$\mathbf{Z}_{\text{MLFMA-FFI}} \cdot \mathbf{I}$ is a recursive version of $\mathbf{Z}_{\text{FMM-FFI}} \cdot \mathbf{I}$. MLFMA always generates a hierarchical tree structure by recursively subdividing the spatial domain. The computational domain is first enclosed in a box; subsequently the box is divided into eight children, where each child is then recursively divided into smaller groups. The recursive division will not stop until the size of the finest box is less than a given size. Detailed explanation of MLFMA can be found in [2].

Similar to $\mathbf{Z}_{\text{FMM-NFI}}$, $\mathbf{Z}_{\text{MLFMA-NFI}}$ is numerically available, which can be written as

$$\mathbf{Z}_{\text{MLFMA-NFI}} = \begin{pmatrix} \mathbf{Z}_{1,1} & \mathbf{Z}_{1,2} & \cdots & 0 \\ \mathbf{Z}_{2,1} & \mathbf{Z}_{2,2} & \cdots & 0 \\ \vdots & \vdots & \cdots & \vdots \\ 0 & \cdots & \mathbf{Z}_{P-1,P-1} & \mathbf{Z}_{P-1,P} \\ 0 & 0 & \mathbf{Z}_{P,P-1} & \mathbf{Z}_{P,P} \end{pmatrix}, \tag{5}$$

where P is the number of nonempty finest MLFMA groups. The actual sparsity pattern of $\mathbf{Z}_{\text{MLFMA-NFI}}$ is determined by near neighbor lists at the finest MLFMA level [2].

2.2. Non-hierarchical ID-MLFMA

The efficiency of MLFMA degrades rapidly for targets with fine meshing because the matrix $\mathbf{Z}_{\text{MLFMA-NFI}}$ heavily depends on the property of the mesh. To circumvent this problem, ID-MLFMA [13] has been proposed by combining the interpolative decomposition (ID) [17] with the conventional MLFMA. Finest MLFMA groups are further decomposed in ID-MLFMA by a recursive manner; the condition for discontinuing the decomposition is based on some predetermined number of basis elements. The ID-MLFMA classifies levels in the resultant oct-tree into three categories: MLFMA levels, the transition level and ID levels. The transition level is identical to the finest MLFMA level. The computations on FFIs at all MLFMA levels are identically conducted by the conventional MLFMA, while those on NFIs at the transition level are conducted through the skeleton approximation at ID levels. In particular, ID-MLFMA classifies NFIs at the transition level into NFIs and FFIs at ID levels; the distinction between the two is based upon the so-called *one-buffer-box* criterion [2].

Suppose

- L_{T}: the transition level (also the finest MLFMA level); here, the 0-th level is the coarsest level;
- L_{ID}: the finest ID level;
- P^L: the number of nonempty groups at the L-th level;
- N_o: the number of unknowns in group o;
- $\mathbf{Z}_{o,s}^{(L)}$: a $N_o \times N_s$ matrix, the coupling matrix of the pair of groups o and s (The superscript L indicates that groups o and s are at the L-th level);
- B_o: near neighbors of group o;
- C_o: children of group o;
- k_o: the number of skeletons in group o;
- $\mathbf{R}_p^{(L)}$: a $k_p \times N_p$ matrix, mapping original sources to their skeletons belonging to group p (The superscript L indicates that group p is at the L-th level);
- $\mathbf{L}_p^{(L)}$: a $N_p \times k_p$ matrix, mapping skeletonized fields to their original forms in group p;
- $\mathbf{S}_{q,p}^{(L)}$: a $k_q \times k_p$ matrix, the skeletonized coupling matrix of the pair of groups q and p at the L-th level.

According to the above nomenclature, $\mathbf{Z}_{\text{MLFMA-NFI}} = \mathbf{Z}_{\text{NFI}}^{(L_{\text{T}})}$, which can be divided into NFIs and FFIs at the $(L_{\text{T}}+1)$-th level as,

$$\mathbf{Z}_{\text{NFI}}^{(L_{\text{T}})} = \mathbf{Z}_{\text{NFI}}^{(L_{\text{T}}+1)} + \mathbf{Z}_{\text{FFI}}^{(L_{\text{T}}+1)}, \tag{6}$$

with

$$\mathbf{Z}_{\text{NFI}}^{(L_{\text{T}}+1)} = \sum_{q} \sum_{p \in B_q} \mathbf{Z}_{q,p}^{(L_{\text{T}}+1)} \tag{7}$$

and

$$\mathbf{Z}_{\text{FFI}}^{(L_{\text{T}}+1)} = \sum_{q} \sum_{p \notin B_q} \mathbf{Z}_{q,p}^{(L_{\text{T}}+1)}, \tag{8}$$

where q, p are nonempty groups at the $(L_{\text{T}}+1)$-th level.

By applying the ID, the FFI submatrix $\mathbf{Z}_{q,p}^{(L_{\text{T}}+1)}$ $(p \notin B_q)$ in (8) can be approximated as [11]

$$\mathbf{Z}_{q,p}^{(L_{\text{T}}+1)} \approx \mathbf{L}_{q}^{(L_{\text{T}}+1)} \cdot \mathbf{S}_{q,p}^{(L_{\text{T}}+1)} \cdot \mathbf{R}_{p}^{(L_{\text{T}}+1)}, \quad p \notin B_q. \tag{9}$$

Substituting (9) into (8) and (6), we can arrive at

$$\begin{aligned} \mathbf{Z}_{\text{NFI}}^{(L_{\text{T}})} &\approx \mathbf{Z}_{\text{NFI}}^{(L_{\text{T}}+1)} + \sum_{q} \sum_{p \notin B_q} \mathbf{L}_{q}^{(L_{\text{T}}+1)} \cdot \mathbf{S}_{q,p}^{(L_{\text{T}}+1)} \cdot \mathbf{R}_{p}^{(L_{\text{T}}+1)} \\ &\approx \mathbf{Z}_{\text{NFI}}^{(L_{\text{T}}+1)} + \mathbf{L}^{(L_{\text{T}}+1)} \cdot \mathbf{S}^{(L_{\text{T}}+1)} \cdot \mathbf{R}^{(L_{\text{T}}+1)}, \end{aligned} \tag{10}$$

where

$$\mathbf{S}^{(L_{\text{T}}+1)} = \begin{pmatrix} 0 & 0 & \dots & \mathbf{S}_{1,P^{L_{\text{T}}+1}}^{(L_{\text{T}}+1)} \\ 0 & 0 & \dots & \mathbf{S}_{2,P^{L_{\text{T}}+1}}^{(L_{\text{T}}+1)} \\ \vdots & \vdots & \ddots & \vdots \\ \mathbf{S}_{P^{L_{\text{T}}+1}-1,1}^{(L_{\text{T}}+1)} & \dots & 0 & 0 \\ \mathbf{S}_{P^{L_{\text{T}}+1},1}^{(L_{\text{T}}+1)} & \dots & 0 & 0 \end{pmatrix}, \tag{11}$$

$$\mathbf{L}^{(L_{\text{T}}+1)} = \begin{pmatrix} \mathbf{L}_{1}^{(L_{\text{T}}+1)} & 0 & \dots & 0 \\ 0 & \mathbf{L}_{2}^{(L_{\text{T}}+1)} & \dots & 0 \\ \vdots & \vdots & \ddots & \vdots \\ 0 & \dots & 0 & \mathbf{L}_{P^{L_{\text{T}}+1}}^{(L_{\text{T}}+1)} \end{pmatrix}. \tag{12}$$

$\mathbf{R}^{(L_{\text{T}}+1)}$ is similarly defined to $\mathbf{L}^{(L_{\text{T}}+1)}$, which is a block diagonal matrix. $\mathbf{Z}_{\text{NFI}}^{(L_{\text{T}}+1)}$ is a sparse matrix similar to $\mathbf{Z}_{\text{MLFMA-NFI}}$ in (5). The sparsity pattern of $\mathbf{S}^{(L_{\text{T}}+1)}$ is determined by that of $\mathbf{Z}_{\text{FFI}}^{(L_{\text{T}}+1)}$.

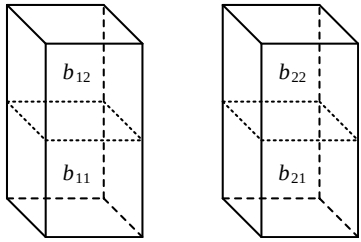

Figure 1. Generating skeletons hierarchically.

The NFI submatrix $\mathbf{Z}_{q,p}^{(L_{\mathrm{T}}+1)}$ in (7) can be further approximated by the ID at the $(L_{\mathrm{T}}+2)$-th level as

$$\mathbf{Z}_{q,p}^{(L_{\mathrm{T}}+1)} \approx \sum_{w\in B_v} \mathbf{Z}_{v,w}^{(L_{\mathrm{T}}+2)} + \sum_{w\notin B_v} \mathbf{L}_v^{(L_{\mathrm{T}}+2)} \cdot \mathbf{S}_{v,w}^{(L_{\mathrm{T}}+2)} \cdot \mathbf{R}_w^{(L_{\mathrm{T}}+2)}, \quad (13)$$

where $v \in C_q$ and $w \in C_p$. Equation (10) then reads

$$\begin{aligned} \mathbf{Z}_{\mathrm{NFI}}^{(L_{\mathrm{T}})} \;\approx\; & \mathbf{Z}_{\mathrm{NFI}}^{(L_{\mathrm{T}}+2)} + \mathbf{L}^{(L_{\mathrm{T}}+2)} \cdot \mathbf{S}^{(L_{\mathrm{T}}+2)} \cdot \mathbf{R}^{(L_{\mathrm{T}}+2)} \\ & + \mathbf{L}^{(L_{\mathrm{T}}+1)} \cdot \mathbf{S}^{(L_{\mathrm{T}}+1)} \cdot \mathbf{R}^{(L_{\mathrm{T}}+1)}. \end{aligned} \quad (14)$$

The procedure through (10) to (14) can be carried out on all ID levels. The MLFMA-NFI matrix can thus be written as

$$\begin{aligned} \mathbf{Z}_{\mathrm{NFI}}^{(L_{\mathrm{T}})} &\approx \mathbf{Z}_{\mathrm{NFI}}^{(L_{\mathrm{ID}})} + \mathbf{L}^{(L_{\mathrm{ID}})} \cdot \mathbf{S}^{(L_{\mathrm{ID}})} \cdot \mathbf{R}^{(L_{\mathrm{ID}})} + \ldots \mathbf{L}^{(L_{\mathrm{T}}+1)} \cdot \mathbf{S}^{(L_{\mathrm{T}}+1)} \cdot \mathbf{R}^{(L_{\mathrm{T}}+1)} \\ &\approx \mathbf{Z}_{\mathrm{NFI}}^{(L_{\mathrm{ID}})} + \sum_{i=L_{\mathrm{T}}+1}^{L_{\mathrm{ID}}} \mathbf{L}^{(i)} \cdot \mathbf{S}^{(i)} \cdot \mathbf{R}^{(i)}. \end{aligned} \quad (15)$$

Hence, $\mathbf{Z}_{\text{MLFMA-NFI}} \cdot \mathbf{I}$ in ID-MLFMA is performed as

$$\mathbf{Z}_{\mathrm{NFI}}^{(L_{\mathrm{T}})} \cdot \mathbf{I} \approx \mathbf{Z}_{\mathrm{NFI}}^{(L_{\mathrm{ID}})} \cdot \mathbf{I} + \sum_{i=L_{\mathrm{T}}+1}^{L_{\mathrm{ID}}} \big(\mathbf{L}^{(i)} \cdot \mathbf{S}^{(i)} \cdot \mathbf{R}^{(i)} \cdot \mathbf{I}\big). \quad (16)$$

Because high rank submatrices corresponding to NFIs at all ID levels are separated from the ID skeletonization, the resultant FFI submatrices in the form of data sparse representation are quite sparse. Therefore, NFIs computed by (16) is much cheaper than by its original form in (4).

3. THE HIERARCHICAL ID-MLFMA

3.1. Conducting ID Skeletonization Hierarchically

In the following, the hierarchical scheme to select skeletons and to construct the corresponding projection matrices are discussed.

Suppose groups b_1 and b_2 are well separated at the $(L-1)$-level. They both have two child groups, denoted by b_{11}, b_{12} and b_{21}, b_{22}, respectively, as shown in Figure 1. The FFI matrix between groups b_1 and b_2 is

$$\begin{aligned}\mathbf{Z}_{1,2}^{(L-!1)} &= \begin{pmatrix} \mathbf{Z}_{11,21}^{(L)} & \mathbf{Z}_{11,22}^{(L)} \\ \mathbf{Z}_{12,21}^{(L)} & \mathbf{Z}_{12,22}^{(L)} \end{pmatrix} = \begin{pmatrix} \mathbf{L}_{11}^{(L)} \cdot \mathbf{S}_{11,21}^{(L)} \cdot \mathbf{R}_{21}^{(L)} & \mathbf{L}_{11}^{(L)} \cdot \mathbf{S}_{11,22}^{(L)} \cdot \mathbf{R}_{22}^{(L)} \\ \mathbf{L}_{12}^{(L)} \cdot \mathbf{S}_{12,21}^{(L)} \cdot \mathbf{R}_{21}^{(L)} & \mathbf{L}_{12}^{(L)} \cdot \mathbf{S}_{12,22}^{(L)} \cdot \mathbf{R}_{22}^{(L)} \end{pmatrix} \\ &= \mathbf{L}_1^{(L)} \cdot \mathbf{S}_{1,2}^{(L)} \cdot \mathbf{R}_2^{(L)}, \end{aligned} \tag{17}$$

where

$$\mathbf{L}_1^{(L)} = \begin{pmatrix} \mathbf{L}_{11}^{(L)} & 0 \\ 0 & \mathbf{L}_{12}^{(L)} \end{pmatrix}, \quad \mathbf{S}_{1,2}^{(L)} = \begin{pmatrix} \mathbf{S}_{11,21}^{(L)} & \mathbf{S}_{11,22}^{(L)} \\ \mathbf{S}_{12,21}^{(L)} & \mathbf{S}_{12,22}^{(L)} \end{pmatrix}, \quad \mathbf{R}_2^{(L)} = \begin{pmatrix} \mathbf{R}_{21}^{(L)} & 0 \\ 0 & \mathbf{R}_{22}^{(L)} \end{pmatrix}.$$

The dense matrix $\mathbf{S}_{1,2}^{(L)}$ can be further approximated by the ID as

$$\mathbf{S}_{1,2}^{(L)} = \mathbf{L}_1^{(L-1)_{\mathrm{h}}} \cdot \mathbf{S}_{1,2}^{(L-1)} \cdot \mathbf{R}_2^{(L-1)_{\mathrm{h}}}. \tag{18}$$

The h in the superscript of $\mathbf{L}_1^{(L-1)_{\mathrm{h}}}$ and $\mathbf{R}_2^{(L-1)_{\mathrm{h}}}$ means that the projection matrices are obtained from the corresponding skeletons instead of the original unknowns. As a result,

$$\begin{aligned}\mathbf{Z}_{1,2}^{(L-1)} &= \mathbf{L}_1^{(L)} \cdot \mathbf{L}_1^{(L-1)_{\mathrm{h}}} \cdot \mathbf{S}_{1,2}^{(L-1)} \cdot \mathbf{R}_2^{(L-1)_{\mathrm{h}}} \cdot \mathbf{R}_2^{(L)} \\ &= \mathbf{L}_1^{(L-1)} \cdot \mathbf{S}_{1,2}^{(L-1)} \cdot \mathbf{R}_2^{(L-1)}, \end{aligned} \tag{19}$$

where

$$\mathbf{L}_1^{(L-1)} = \mathbf{L}_1^{(L)} \cdot \mathbf{L}_1^{(L-1)_{\mathrm{h}}}, \quad \mathbf{R}_2^{(L-1)} = \mathbf{R}_2^{(L-1)_{\mathrm{h}}} \cdot \mathbf{R}_2^{(L)}.$$

After carrying out the skeletonization procedure (19)on all FFI submatrices at the $(L-1)$-th level, the resultant FFI matrix reads

$$\mathbf{Z}_{\mathrm{FFI}}^{(L-1)} = \mathbf{L}^{(L-1)} \cdot \mathbf{S}^{(L-1)} \cdot \mathbf{R}^{(L-1)}, \tag{20}$$

where

$$\mathbf{L}^{(L-1)} = \mathbf{L}^{(L)} \cdot \mathbf{L}^{(L-1)_{\mathrm{h}}}, \quad \mathbf{R}^{(L-1)} = \mathbf{R}^{(L-1)_{\mathrm{h}}} \cdot \mathbf{R}^{(L)}. \tag{21}$$

$\mathbf{L}^{(L)}$, $\mathbf{R}^{(L-1)_{\mathrm{h}}}$, $\mathbf{R}^{(L)}$ and $\mathbf{R}^{(L-1)_{\mathrm{h}}}$ in (21) are all block diagonal matrices having the similar definition to $\mathbf{L}^{(L_{\mathrm{T}}+1)}/\mathbf{R}^{(L_{\mathrm{T}}+1)}$ in (12).

(18) and (20) show the essence of the hierarchical scheme to select skeletons. In particular, after projection matrices $\mathbf{L}^{(L_{\mathrm{ID}})}$ and $\mathbf{R}^{(L_{\mathrm{ID}})}$ at the finest ID level are generated, projection matrices at the L-th level

can be computed by a recursive manner as

$$\mathbf{L}^{(L)}=\mathbf{L}^{(L_{\mathrm{ID}})}\cdot\mathbf{L}^{(L_{\mathrm{ID}}-1)_{\mathrm{h}}}\cdot,\ldots,\cdot\mathbf{L}^{(L)_{\mathrm{h}}}=\mathbf{L}^{(L_{\mathrm{ID}})}\cdot\left(\prod_{i=L_{\mathrm{ID}}-1}^{L}\mathbf{L}^{(i)_{\mathrm{h}}}\right), \quad (22)$$

$$\mathbf{R}^{(L)}=\mathbf{R}^{(L)_{\mathrm{h}}}\cdot,\ldots,\cdot\mathbf{R}^{(L-1)_{\mathrm{h}}}\cdot\mathbf{R}^{(L_{\mathrm{ID}})}=\left(\prod_{i=L}^{L_{\mathrm{ID}}-1}\mathbf{R}^{(i)_{\mathrm{h}}}\right)\cdot\mathbf{R}^{(L_{\mathrm{ID}})}. \quad (23)$$

By making use of (22) and (23), the MLFMA-NFI matrix in (6) can be written as

$$\mathbf{Z}_{\mathrm{NFI}}^{(L_{\mathrm{T}})}\approx\mathbf{Z}_{\mathrm{NFI}}^{(L_{\mathrm{ID}})}+\sum_{i=L_{\mathrm{T}}+1}^{L_{\mathrm{ID}}}\left(\mathbf{L}^{(L_{\mathrm{ID}})}\cdot\prod_{m=L_{\mathrm{ID}}}^{i}\mathbf{L}^{(m)_{\mathrm{h}}}\cdot\mathbf{S}^{(i)}\cdot\prod_{m=i}^{L_{\mathrm{ID}}}\mathbf{R}^{(m)_{\mathrm{h}}}\cdot\mathbf{R}^{(L_{\mathrm{ID}})}\right). \quad (24)$$

In (24), $\mathbf{L}^{(L_{\mathrm{ID}})_{\mathrm{h}}}$ and $\mathbf{R}^{(L_{\mathrm{ID}})_{\mathrm{h}}}$ are unit matrices.

3.2. Implementing MVM Hierarchically

According to (24), MVM in the hierarchical ID-MLFMA can be carried out as

$$\mathbf{Z}_{\mathrm{NFI}}^{(L_{\mathrm{T}})}\cdot\mathbf{I}\approx\mathbf{Z}_{\mathrm{NFI}}^{(L_{\mathrm{ID}})}\cdot\mathbf{I}+\sum_{i=L_{\mathrm{T}}+1}^{L_{\mathrm{ID}}}\left(\mathbf{L}^{(L_{\mathrm{ID}})}\cdot\prod_{m=L_{\mathrm{ID}}}^{i}\mathbf{L}^{(m)_{\mathrm{h}}}\cdot\mathbf{S}^{(i)}\cdot\prod_{m=i}^{L_{\mathrm{ID}}}\mathbf{R}^{(m)_{\mathrm{h}}}\cdot\mathbf{R}^{(L_{\mathrm{ID}})}\cdot\mathbf{I}\right). \quad (25)$$

Compared with the MVM in the form of (16), the one based on (25) is generally more efficient. Suppose the well-separated groups g_1 and g_2 are at the L-th level. Further assume:

- both groups g_1 and g_2 have 4096 unknowns;
- both groups g_1 and g_2 have 256 skeletons, which are referred to as skeletons at the L-th level;
- both groups g_1 and g_2 have eight children at the $(L+1)$-th level;
- unknowns and skeletons (at the L-th level) of groups g_1 and g_2 are both evenly distributed across their 8 children;
- each child group has 128 skeletons, which are referred to as skeletons at the $(L+1)$-th level;
- using the approach described in (22) and (23), the same two sets of 256 skeletons can be selected for groups g_1 and g_2, where each child contributes 32 skeletons to its parent.

Therefore, the MVM needs $262,144 = (2 \times 128 \times 512 \times 8 + 2 \times 32 \times 128 \times 8 + 256 \times 256)$ operations by the hierarchical strategy in (25). In contrast, it requires $2,162,688 = (2 \times 256 \times 4096 + 256 \times 256)$ operations through the approach described in (16). Obviously, the MVM is more efficiently performed by (25) than by (26).

4. REDUCING THE SIZE OF THE LOW-RANK MATRIX

To cut down the cost of ID skeletonization, reducing the size of the $\mathbf{Z}_{\mathrm{LR}}$ matrix is always beneficial. Here, the $\mathbf{Z}_{\mathrm{LR}}$ matrix is referred to the low-rank matrix to which the ID is applied in the skeletonization procedure. In this section, an efficient strategy to reduce the size of $\mathbf{Z}_{\mathrm{LR}}$ is developed by making use of the obtained skeletons.

The two approaches to generate $\mathbf{Z}_{\mathrm{LR}}$, namely, *O-FFI matrix* approach and the *AS matrix* one, have been studied and compared comprehensively in [11]. The O-FFI matrix approach is to generate $\mathbf{Z}_{\mathrm{LR}}$ associated with a given group by concatenating all FFI submatrices of this group. The AS matrix approach is to obtain $\mathbf{Z}_{\mathrm{LR}}$ based on the MoM interaction matrix between the group of interest and a sufficient large artificial sphere enclosing this group. If the O-FFI matrix approach is used, $\mathbf{Z}_{\mathrm{LR}}$ is a $(2 \times N_q) \times N_{\mathrm{tot}}$ matrix for group q, where $N_{\mathrm{tot}} = \sum_{p \notin B_q} N_p$. In contrast, $\mathbf{Z}_{\mathrm{LR}}$ becomes a $(2 \times N_q) \times N_a$ matrix in the AS matrix approach, where N_a is the number of unknowns to discretize the artificial sphere. In general, $N_a \ll N_{\mathrm{tot}}$, especially when the ID group q is small in size. Therefore, the AS matrix approach is far more efficient than its O-FFI counterpart because the second dimension of $\mathbf{Z}_{\mathrm{LR}}$ is cut down a lot.

The AS matrix approach can be revised into its skeletonized variation in hierarchical ID-MLFMA, denoted by the skeletonized AS (S-AS) matrix approach. The S-AS approach generates $\mathbf{Z}_{\mathrm{LR}}$ for group q according to skeletons of q's children instead of original unknowns in q. As a result, $\mathbf{Z}_{\mathrm{LR}}$ will become a $(2 \times N'_q) \times N_a$ matrix, where $N'_q = \sum_{v \in C_q} k_v$. Since N'_q is generally much smaller than N_q, the size of $\mathbf{Z}_{\mathrm{LR}}$ is reduced. If group q locates at the finest ID level, $N'_q = N_q$.

A recursive version of the O-FFI matrix approach, denoted as the skeletonized FFI (S-FFI) matrix approach, can be similarly developed in hierarchical ID-MLFMA. Particularly, the S-FFI matrix approach concatenates skeletonized submatrices $\mathbf{S}_{v,w}^{(L+1)}$ and $(\mathbf{S}_{w,v}^{(L+1)})^H$ instead of their original counterpart to generate $\mathbf{Z}_{\mathrm{LR}}$ for group q, where $v \in C_q$, $w \in C_p$ and $p \in B_q$. Therefore, the first dimension of $\mathbf{Z}_{\mathrm{LR}}$ becomes

$2 \times N'_q$ and the second one is reduced to $N'_{\text{tot}} = \sum_{p \in B_q} \sum_{w \in C_p} k_w$. If $N'_{\text{tot}} \ll N_{\text{tot}}$, the size of $\mathbf{Z}_{\text{LR}}$ is much smaller than that generated by the O-FFI approach.

The relationship between N'_{tot} and N_a is application dependent. For higher efficiency, a mixed approach to generate $\mathbf{Z}_{\text{LR}}$ is designed here by combining together S-AS and S-FFI matrix approaches. The mixed strategy is

$$\begin{cases} \text{S-AS matrix approach}, & \text{if } N_a \leq N'_{\text{tot}}; \\ \text{S-FFI matrix approach}, & \text{else.} \end{cases}$$

It is worthy pointing out that the MLFMA aggregation and disaggregation matrices can also be skeletonized. The skeletons at L_{T+1}-th level can be used to generate $\mathbf{Z}_{\text{LR}}$ in the skeletonization procedure. Since our experience shows that the FFI is much cheaper than NFI in MLFMA for multiscale applications, we focus on the MLFMA-NFI here. The aggregation and disaggregation matrices are obtained from the original unknowns at the L_T-th level as in the traditional MLFMA.

5. NUMERICAL RESULTS

The following numerical experiments are carried out on an IBM sever configured by X5650 CPU and 64 GB memory. In all computations, 6 threads are forked to conduct OpenMP parallelization as one CPU has 6 cores. RWG functions are chosen as basis and testing functions to discretize CFIE with a combination coefficient of 0.5. The GMRES iteration process accelerated by an ILU-typed preconditioner is terminated when the L^2-norm of the residual vector is reduced to 10^{-3}. ε is set to 10^{-3} in the skeleton selection procedure.

In this section, notations are defined as follows:

- $T_{\text{NFI}}^{(L)}$ and $M_{\text{NFI}}^{(L)}$ are the CPU time to filling and the memory requirement of all original NFI block matrices ($\mathbf{Z}_{o,s}^{(L)}(s \in B_o)$) at the L-th level;
- T_{proj} and M_{proj} are the CPU time to filling and the memory requirement of projection matrices $\mathbf{R}/\mathbf{L}$ at all ID levels;
- T_{samp} and M_{samp} are the CPU time to filling and the memory requirement of sampling matrices $\mathbf{S}$ at all ID levels;
- $T_{\text{NFI}}^{\text{ID}} = T_{\text{NFI}}^{(L_{\text{ID}})} + T_{\text{proj}} + T_{\text{samp}}$ and $M_{\text{NFI}}^{\text{ID}} = M_{\text{NFI}}^{(L_{\text{ID}})} + M_{\text{proj}} + M_{\text{samp}}$;
- T_{MVM} and T_{itr} are the CPU time for $\mathbf{Z}_{\text{NFI}}^{(L_{\text{T}})} \cdot \mathbf{I}$ in one MVM, the CPU time for iteration and the total solution;

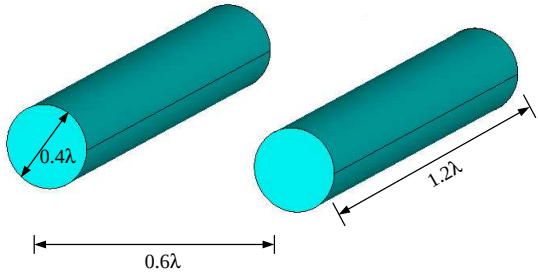

Figure 2. The two-cylinder target.

- T_{tot} and M_{tot} are the CPU time and memory for the total solution;
- $\delta_{\text{MVM}} = \frac{\|f_{\text{ref}} - f_{\text{ID}}\|}{\|f_{\text{ref}}\|}$, where f_{ID} is the MVM result obtained by the ID approximation, f_{ref} is the exact MVM result without approximation, and $\|\cdot\|$ is the Euclidean norm.

5.1. The Two-cylinder Target

A two-cylinder target, as shown in Figure 2, is used to validate the accuracy and efficiency of the proposed hierarchical ID-MLFMA.

The two cylinders are identical in dimensions. The mesh of the target is highly non-uniform where the two cylinders are, respectively, discretized with an average mesh size of 0.05λ and 0.005λ. The total number of unknowns is 114,060. In the computations, the finest MLFMA group size is set to be 0.3λ. Consequently, the finest MLFMA level is the 2-nd level. $\mathbf{Z}_{\text{NFI}}^{(2)}$, the MLFMA-NFI matrix, costs 62.0 GB memory and 19,832 s. The memory required by MLFMA-FFI is about 135 MB. T_{MVM} in MLFMA is 22.4 s, while MLFMA-FFI in one MVM costs 0.5 s. Because $\mathbf{Z}_{\text{NFI}}^{(2)}$ consumes all the memory available and no preconditioner can be constructed, the iteration in the MLFMA computation fails to converge to 10^{-3}.

Table 1 shows statistics in the non-hierarchical ID-MLFMA computation. The finest ID level is the 6-th level. $\mathbf{Z}_{\text{NFI}}^{(6)}$ consumes 453 MB memory, while $\mathbf{S}^{(i)}$ matrices at all ID levels require over 8.5 GB memory in total. The ID skeletonization approximation reduces the memory requirement by a factor of 6.0.

The proposed hierarchical scheme can improve the efficiency of ID-MLFMA, especially when the mixed strategy is employed to generate $\mathbf{Z}_{\text{LR}}$ matrices in the skeletonization procedure. Table 2 presents the statistics when different strategies of generating $\mathbf{Z}_{\text{LR}}$ in the hierarchical ID-MLFMA. As indicated in this table, when S-AS strategy is used, a smaller number of skeletons are required in comparison with the non-

hierarchical computation. The memory requirement of $\mathbf{S}^{(i)}$ matrices is thus cut down to 6.2 GB. The CPU time for one MVM is decreased from 2.8 s to 1.0 s. The ID skeletonization is accelerated as well, whose

Table 1. Computational statistics for the two-cylinder target in the non-hierarchical ID-MLFMA computation where the artificial sphere strategy is used to generate $\mathbf{Z}_{\mathrm{LR}}$ (T_{tot} does not include the cost of the preconditioner).

Skeleton #	6-th level	89918
	5-th level	53186
	4-th level	56726
	3-th level	3011
Memory (MB)	$M_{\mathrm{NFI}}^{(6)}$	453
	M_{proj}	150
	M_{samp}	8582
	M_{tot}	9320
Time (s)	T_{proj}	620
	T_{samp}	2479
	T_{MVM}	2.8
	T_{itr}	2931
	T_{tot}	6031
δ_{MVM} ($\times 10^{-3}$)		0.6

Table 2. Computational statistics for the two-cylinder target when different strategies used to generate $\mathbf{Z}_{\mathrm{LR}}$ matrices in the hierarchical ID-MLFMA (T_{tot} does not include the cost of the preconditioner).

		S-AS	S-FFI	Mixed
Skeleton #	6-th level	89918	89918	89918
	5-th level	48186	34700	35192
	4-th level	42739	24627	25150
	3-th level	2933	2219	2265
Memory (MB)	M_{proj}	12	13	12
	M_{samp}	6231	2511	2607
	M_{tot}	6831	3112	3207
Time (s)	T_{proj}	459	2530	1201
	T_{samp}	1346	3	220
	T_{MVM}	1.0	0.6	0.6
	T_{itr}	1260	713	721
	T_{tot}	3065	3246	2142
δ_{MVM} ($\times 10^{-3}$)		0.6	0.6	0.6

cost, obtained by $T_{\text{proj}} + T_{\text{samp}}$, is reduced from 3099 s to 1805 s.

The S-FFI strategy can improve the efficiency by furtherly reducing the number of skeletons. For example, the memory requirement of $\mathbf{S}^{(i)}$ matrices is cut down to 2.5 GB from 6.2 GB in the S-AS case. The time for each MVM is reduced from 1.0 s to 0.6 s. But, the time to conduct the ID skeletonization, $T_{\text{proj}} + T_{\text{samp}}$, is increased to 2533 s from 1805 s in the S-AS case because of the high cost of filling FFI matrices. Fortunately, the mixed strategy can overcome this problem by the smart alteration between the S-AS and the S-FFI strategies. As shown in Table 2, the mixed strategy successfully reduces the CPU time of the ID skeletonization procedure from 2533 s to 1421 s. The cost of this mixed strategy is the negligible increase of the number of skeletons in comparison with the S-FFI case. It should be noted that, in the S-FFI case, we obtain all $\mathbf{S}$ matrices from its corresponding FFI matrices. So, little time is used to fill $\mathbf{S}$ matrices.

Iterations in all ID-MLFMA computations converge in 60 steps with the ILU-typed preconditioner. Since we focus on the proposed hierarchical scheme for ID skeletonization, the time to construct the preconditioner isn't included in T_{tot}. As shown in Tables 1 and 2, δ_{MVM} in all cases are less than 10^{-3}.

5.2. The F117 Aircraft Model

Numerical experiments are carried out on the F117 aircraft model to show the capability of the hierarchical ID-MLFMA on the target with a complex shape. The model is discretized by 106,965 unknowns. The longest, shortest and average edge lengthes are about 0.05λ, 0.0003λ and 0.016λ. We compare the proposed hierarchical ID-MLFMA with the traditional MLFMA and the non-hierarchical ID-

Table 3. Computational statistics for F117 aircraft model when traditional MLFMA and ID-MLFMA are employed (T_{tot} does not include the cost of the preconditioner).

	MLFMA	ID-MLFMA	
		Non-hier	Hier
$M_{\text{NFI}}^{(3)}/M_{\text{NFI}}^{\text{ID}}$ (MB)	30593	5182	3565
M_{tot}	30815	5404	3787
$T_{\text{NFI}}^{(3)}/T_{\text{NFI}}^{\text{ID}}$ (s)	2305	1535	759
T_{MVM} (s)	2.3	1.2	0.6
T_{itr} (s)	233	125	61
T_{tot} (s)	2538	1660	820
δ_{MVM} ($\times 10^{-3}$)	-	0.9	0.9

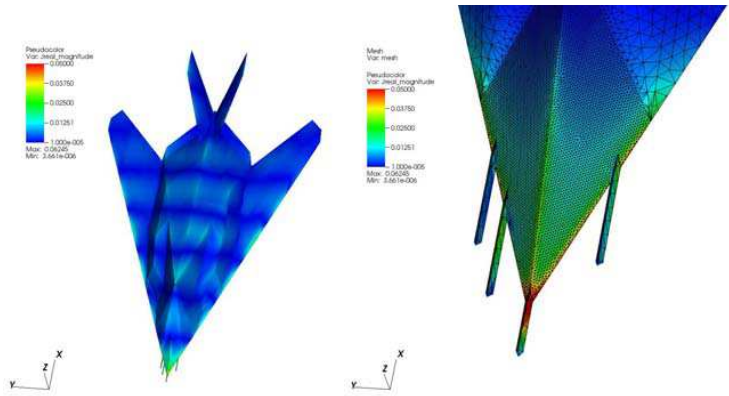

(a) (b)

Figure 3. Current distribution of F117 model under the incident of (60°, 0°). (a) Full view. (b) Detailed view.

MLFMA. The finest MLFMA and ID level is respectively the 3-rd and 8-th level. In the hierarchical ID-MLFMA computation, the mixed strategy of generating low-rank matrices to conduct ID skeletonization is employed.

Table 3 lists statistics on computational resources. $\mathbf{Z}_{\mathrm{NFI}}^{(3)}$, the NFI matrix in MLFMA, costs about 31.0 GB memory and 2,305 s. The memory required by MLFMA-FFI is about 222 MB. T_{MVM} in MLFMA is 2.3 s, while MLFMA-FFI in one MVM costs 0.6 s. An ILU-typed preconditioner is applied to make the iterations converge in less then 60 steps as the unpreconditioned iterations in both MLFMA and ID-MLFMA computations do not converge in 500 steps. The non-hierarchical ID-MLFMA approximates $\mathbf{Z}_{\mathrm{NFI}}^{(3)}$ by 5.1 GB memory. The proposed hierarchical scheme furtherly improves efficiency of ID-MLFMA. Particularly, the hierarchical ID-MLFMA approximates the $\mathbf{Z}_{\mathrm{NFI}}^{(3)}$ matrix by 3.5 GB. The cost of the ID skeletonization procedure is decreased from 1535 s to 759 s. Additionally, T_{MVM} is also cut down by a factor of 2.0. Figure 3 presents the computed current under the incident of (60°, 0°). The Euclidean norm of the difference between the current obtained by MLFMA and those by ID-MLFMA is less than 3.0×10^{-3}.

6. CONCLUSIONS

Based on the proposed hierarchical schemes on conducting ID skeletonization and implementing matrix vector multiplication, a new

interpolative decomposition multilevel fast multipole algorithm (ID-MLFMA) is proposed to handle multiscale, dynamic electromagnetic problems. The mixed strategy to reduce the size of low-rank matrices is developed to improve efficiency of ID skeletonization. Numerical experiments reveal that the proposed hierarchical scheme in connection with the mixed strategy of generating low-rank matrices improves the efficiency of ID-MLFMA. Computations on the F117 aircraft model demonstrate the capability of the hierarchical ID-MLFMA on multiscale problems.

ACKNOWLEDGMENT

This work was supported by the NSFC under Grant 10832002, by the NSFC under Grant 60901005, by the Excellent Scholars Support Fund of Beijing under Grant 2012D009011000002.

REFERENCES

1. Coifman, R., V. Rokhlin, and S. Wandzura, "The fast multipole method for the wave equation: A pedestrian prescription," *IEEE Antennas and Propag. Mag.*, Vol. 35, No. 3, 7–12, 1993.
2. Chew, W. C., J. M. Jin, E. Michielssen, and J. Song, *Fast Efficient Algorithms in Computational Electromagnetics,* Artech House, Boston, MA, 2001.
3. Yuan, N., T. S. Yeo, X. C. Nie, L. W. Li, and Y. B. Gan, "Analysis of scattering from composite conducting and dielectric targets using the precorrected-FFT algorithm," *Journal of Electromagnetic Waves and Applications*, Vol. 17, No. 3, 499–515, 2003.
4. Garcia, E., C. Delgado, L. Lozano, I. Gonzalez-Diego, and M. F. Catedra, "An efficient hybrid-scheme combining the characteristic basis function method and the multilevel fast multipole algorithm for solving bistatic RCS and radiation problems," *Progress In Electromagnetics Research B*, Vol. 34, 327–343, 2011.
5. Lai, B., H. B. Yuan, and C.-H. Liang, "Analysis of nurbs surfaces modeled geometries with higher-order mom based AIM," *Journal of Electromagnetic Waves and Applications*, Vol. 25, Nos. 5–6, 683–691, 2011.
6. Pan, X.-M., W.-C. Pi, and X.-Q. Sheng, "On openmp parallelization of the multilevel fast multipole algorithm," *Progress In Electromagnetics Research*, Vol. 112, 199–213, 2011.

7. Shao, H., J. Hu, Z.-P. Nie, G. Han, and S. He, "Hybrid tangential equivalence principle algorithm with MLFMA for analysis of array structures," *Progress In Electromagnetics Research*, Vol. 113, 127–141, 2011.
8. Ergul, O., "Parallel implementation of MLFMA for homogeneous objects with various material properties," *Progress In Electromagnetics Research*, Vol. 121, 505–520, 2011.
9. Pan, X. M., W. C. Pi, M. L. Yang, Z. Peng, and X. Q. Sheng, "Solving problems with over one billion unknowns by the MLFMA," *IEEE Trans. Antennas Propag.*, Vol. 60, No. 5, 2012.
10. Schobert, D. T. and T. F. Eibert, "Fast integral equation solution by multilevel Green's function interpolation combined with multilevel fast multipole method," *IEEE Trans. Antennas Propag.*, Vol. 60, No. 9, 4458–4463, 2012.
11. Wulf, D. and R. Bunger, "An efficient implementation of the combined wideband MLFMA/LF-FIPWA," *IEEE Trans. Antennas Propag.*, Vol. 57, No. 12, 467–474, 2009.
12. Bogaert, I., J. Peeters, and F. Olyslager, "A nondirective plane wave MLFMA stable at low frequencies," *IEEE Trans. Antennas Propag.*, Vol. 56, No. 12, 3752–3767, 2008.
13. Pan, X. M., J. G. Wei, Z. Peng, and X. Q. Sheng, "A fast algorithm for multiscale electromagnetic problems using interpolative decomposition and multilevel fast multipole algorithm," *Radio Sci.*, Vol. 47, 2012.
14. Greengard, L., D. Gueyffier, P. G. Martinsson, and V. Rokhlin, "Fast direct solvers for integral equations in complex three-dimensional domains," *Acta Numerica*, Vol. 18, 243–275, 2009.
15. Ho, K. L. and L. Greengard, "A fast direct solver for structured linear systems by recursive skeletonization," *SIAM J. Sci. Comput.*, Vol. 34, No. 5, A2507–A2532, 2012.
16. Rodriguez, J. L., J. M. Taboada, M. G. Araujo, F. O. Basteiro, L. Landesa, and I. Garcia-Tunon, "On the use of the singular value decomposition in the fast multipole method," *IEEE Trans. Antennas Propag.*, Vol. 56, No. 8, 2325–2334, 2008.
17. Liberty, E., F. Woolfe, P. G. Martinsson, V. Rokhlin, and M. Tygert, "Randomized algorithms for the low-rank approximation of matrices," *Proc. Natl. Acad. Sci.*, Vol. 104, 20167–20172, US, 2007.